Molecular Bases of Disease:

A Pre-microRNA-149 (miR-149) Genetic Variation Affects miR-149 Maturation and Its Ability to Regulate the Puma Protein in Apoptosis

Su-Ling Ding, Jian-Xun Wang, Jian-Qin Jiao, Xin Tu, Qing Wang, Fang Liu, Qian Li, Jie Gao, Qun-Yong Zhou, Dong-Feng Gu and Pei-Feng Li

J. Biol. Chem. 2013, 288:26865-26877.
doi: 10.1074/jbc.M112.440453 originally published online July 19, 2013

THE JOURNAL OF BIOLOGICAL CHEMISTRY VOL. 288, NO. 37, pp. 26865–26877, September 13, 2013

A Pre-microRNA-149 (miR-149) Genetic Variation Affects miR-149 Maturation and Its Ability to Regulate the Puma Protein in Apoptosis*◆

Received for publication, November 28, 2012, and in revised form, July 10, 2013 Published, JBC Papers in Press, July 19, 2013, DOI 10.1074/jbc.M112.440453

Su-Ling Ding[‡], Jian-Xun Wang[‡], Jian-Qin Jiao[‡], Xin Tu[§], Qing Wang[§], Fang Liu[‡], Qian Li[‡], Jie Gao[‡], Qun-Yong Zhou[¶], Dong-Feng Gu[‖1], and Pei-Feng Li[‡2]

From the [‡]Division of Cardiovascular Research, State Key Laboratory of Biomembrane and Membrane Biotechnology, Institute of Zoology, Chinese Academy of Sciences, Beijing 100101, China, the [§]Key Laboratory of Molecular Biophysics of the Ministry of Education, Center for Human Genome Research, College of Life Science and Technology, Huazhong University of Science and Technology, Wuhan 430074, China, the [¶]Department of Pharmacology, University of California, Irvine, California 92697, and the [‖]State Key Laboratory of Cardiovascular Disease, Fuwai Hospital, National Center of Cardiovascular Diseases, Chinese Academy of Medical Sciences and Peking Union Medical College, Beijing 100037, China

Background: The role of miRNA SNPs in disease susceptibility remains ill-defined.
Results: The polymorphism rs71428439 is associated with the risk for myocardial infarction and affects miR-149 maturation. Puma is a target of miR-149.
Conclusion: This polymorphism contributes to the risk of myocardial infarction through the miR-149-Puma axis.
Significance: This polymorphism, miR-149, and Puma can be targets for the development of individualized treatment for myocardial infarction.

MicroRNAs (miRNAs) are small, single-stranded, noncoding RNAs that function as negative regulators of gene expression. They are transcribed from endogenous DNA and form hairpin structures (termed as pre-miRNAs) that are processed to form mature miRNAs. It remains largely unknown as to the molecular consequences of the natural genetic variation in pre-miRNAs. Here, we report that an A→G polymorphism (rs71428439) is located in *Homo sapiens* miR-149 stem-loop region. This polymorphism results in a change in the structure of the miR-149 precursor. Our results showed that the genotype distribution of this polymorphism in myocardial infarction cases was significantly different from that in the control subjects. We examined the biological significance of this polymorphism on the production of mature miR-149, and we observed that the G-allelic miR-149 precursor displayed a lower production of mature miR-149 compared with the A-allelic one. Further investigations disclosed that miR-149 could withstand mitochondrial fission and apoptosis through targeting the pro-apoptotic factor p53-up-regulated modulator of apoptosis (Puma). Enforced expression of miR-149 promoted cell survival, whereas knockdown of miR-149 rendered cells to be sensitive to apoptotic stimulation. Intriguingly, the A to G variation led pre-miR-149 to elicit an attenuated effect on the inhibition of mitochondrial fission and apoptosis. Finally, this polymorphism exerts its influence on cardiac function in the mouse model of myocardial infarction. These data suggest that this polymorphism in the miR-149 precursor may result in important phenotypic traits of myocardial infarction. Our findings warrant further investigations on the relationship between miR-149 polymorphism and myocardial infarction.

Myocardial infarction (MI),[3] one of the complex diseases harmful to human health and life, is the result of interaction between genetic and environmental factors. Its pathogenesis needs to be fully elucidated. The heritability component of myocardial infarction has been extensively reevaluated in the last few years by genome-wide association studies (1–5), but those studies mainly focused on protein-coding genes and their promoters.

MicroRNAs (miRNAs) are small, single-stranded, noncoding RNAs of about 22 nucleotides that function as negative regulators of the expression of protein-coding genes (6). They are transcribed from endogenous DNA and form hairpin structures (called pre-microRNAs) that are processed to form mature miRNAs. RNA-induced silencing complex facilitates the coupling of mature miRNAs with matching mRNA sequences in the 3′-untranslated regions (3′UTR) through base complementarity. Upon binding to mRNA, the microRNAs partially inhibit the mRNA translation or promote mRNA degradation, thereby disturbing the normal expression of the proteins.

Thousands of miRNA molecules have been reported in the human genome that play key roles in a broad range of physio-

* This work was supported by National Natural Science Foundation of China Grants 31010103911 and 81230005, National Basic Research Program of China, 973 Program Grant 2011CB965300, and Overseas, Hong Kong and Macao Scholars Collaborated Researching Fund 81128002, H0203.
◆ This article was selected as a Paper of the Week.
[1] To whom correspondence may be addressed. E-mail: gudongfeng@vip.sina.com.
[2] To whom correspondence may be addressed. E-mail: peifli@ioz.ac.cn.

[3] The abbreviations used are: MI, myocardial infarction; miRNA, microRNA; pre-miRNA, miRNA precursor; SNP, single nucleotide polymorphisms; Puma, p53-up-regulated modulator of apoptosis; m.o.i., multiplicity of infection; qRT-PCR, quantitative reverse transcription-PCR; OR, odds ratio; CI, confidence interval.

logical and pathological processes, including development, apoptosis, cell proliferation, hematopoiesis, and tumorigenesis (7–10). A growing number of studies have demonstrated that the aberrant expression of miRNAs was closely related to the etiology, diagnosis, and prognosis of many diseases, including heart diseases (11).

Single nucleotide polymorphisms (SNP) in protein-coding genes have been confirmed to link to many kinds of diseases. Although the role of miRNA SNPs in disease susceptibility remains largely unknown, its importance has been greatly implicated in many cancers such as thyroid cancer (12), renal cell carcinoma (13), and breast cancer (14). It is evident that common SNPs in miRNAs and SNPs within their targets may affect miRNA target expression and functions (12, 15). Moreover, SNPs in miRNAs have been demonstrated to affect the miRNA expression (12, 16). Recently, it was reported that a naturally occurring miR-499 mutation outside the critical seed sequence modifies mRNA targeting and end-organ function of miR-499 (17). All these studies suggest that the sequence variation caused by SNP or mutation may greatly contribute to the heterogeneity of complex diseases.

This study conducted a systematic search of SNPs within pre-miRNAs that have been verified to express in the heart (11, 18–20). We found that an A→G polymorphism (rs71428439) identified in the miR-149 gene is associated with the risk of myocardial infarction. This polymorphism is located in the stem region outside the mature miR-149 sequence and results in a change to the structure of the miR-149 precursor. Intriguingly, we observed that the G-allelic miR-149 precursor displayed a low efficiency to produce mature miR-149 compared with the A-allelic one. In follow-up functional analysis, our results showed that the miR-149 suppressed apoptosis through targeting the pro-apoptotic protein Puma. The A to G variation caused by the SNP in the miR-149 precursor leads to a reduced effect of pre-miR-149 to inhibit Puma expression and the consequent apoptosis. Our results warrant future studies to explore this SNP of pre-miR-149 in the pathophysiology of myocardial infarction.

EXPERIMENTAL PROCEDURES

Study Subjects—All study subjects were Han people enrolled from Hubei Province in China. The diagnosis of myocardial infarction was based on the following criteria: 1) typical chest pain lasting longer than 30 min; 2) characteristic electrocardiographic patterns of myocardial infarction; 3) elevation of cardiac enzymes (creatine kinase and lactate dehydrogenase), and troponin I or T in blood. The control individuals were randomly selected and matched to cases based on age and gender. Hypertension was defined as receiving ongoing medication for hypertension, systolic blood pressure ≥140 mm Hg, or diastolic blood pressure ≥90 mm Hg. Diabetes mellitus was defined as ongoing therapy for diabetes or a fasting plasma glucose level ≥7.0 mM/liter. The investigations complied with the ethical guidelines of the 1975 Declaration of Helsinki and were approved by appropriate local institutional review boards on human subject research. Informed consent was obtained from all participants.

Genotyping—Genomic DNA was extracted from peripheral blood samples. Genotypes were analyzed by polymerase chain reaction (PCR)-based direct DNA sequencing. DNA specimens were amplified by using standard PCR protocols. The PCR products were purified and sequenced in both directions. The sequencing results were analyzed by using DNAStar SEQMAN software. The primers, 5′-TCTCATGTCCAGGACCACAA-3′ and 5′-GAGAGGCATGGAGAGGTGAG-3′, were used to amplify a 493-bp fragment covering the A→G polymorphism site (rs71428439) in the miR-149 precursor.

Cell Cultures, Hydrogen Peroxide Treatment—Primary mouse cardiomyocytes were isolated from hearts of 1-day-old mouse pups, as we described elsewhere (21), with minor modifications. Briefly, non-myocyte contaminants were removed by two rounds of pre-plating for 1.5 h on 100-mm plastic cell culture dishes in a humidified incubator at 37 °C with 5% CO_2. Cardiomyocytes were plated separately into 24-well culture plates or 60-mm culture dishes with serum-containing medium. Following a 24-h incubation period, serum-containing medium was replaced with no serum medium. The treatment with hydrogen peroxide was performed as we described (22).

Construction of miR-149 Expression Vectors—To create the allelic A and G pre-miR-149 expression vectors separately, the 493-bp DNA fragments encompassing the miR-149 precursor sequence and its 5′- and 3′-flanking regions (199 and 205 bp, respectively) were amplified from human genomic DNA from normal blood donors (determined to have the AA or GG genotype) and cloned into the XhoI and XbaI sites of the vector pcDNA3 (Invitrogen). The sequences of both vectors were confirmed by direct sequencing, and the only difference was in the SNP. The yielded vector with the AA genotype was designated pc3.0-miR-149-A, and the one with the GG genotype was named pc3.0-miR-149-G. pc3.0-miR-423, which contained the miR-423 precursor sequence and its 5′- and 3′-flanking regions (253 and 117 bp, respectively), and pc-3.0-cel-miR-39, which contained cel-miR-39 precursor and its 5′- and 3′-flanking regions (85 and 195 bp separately), were constructed as negative controls.

Production of miR-149 Duplex or Inhibitor—Chemically modified antagomir reverse complementary to miR-149 was used to inhibit its expression. The miR-149 antagomir (As-miR-149) sequence was 5′-GGGAGUGAAGACACGGAGCCAGA-3′. Chemically modified oligonucleotide 5′-CAGUACUUUUGUGUAGUACAA-3′ was used as antagomir negative control (designated as As-NC). All of the bases were 2′-OMe modified. miR-149 mimic (designated as miR-149), designed as described elsewhere (23), was employed to enhance its expression. It contains an RNA strand with the sequence identical to the mature miR-149 and an artificial strand that was partially complementary to the mature miR-149 sequence. The miR-149 antagomir and mimic used in this study were both synthesized by GenePharma Co. Ltd. miRNA duplexes (sense, 5′-UUCUCCGAACGUGUCACGUTT-3′; antisense, 5′-ACGUGACACGUUCGGAGAATT-3′) were used as a negative control (designated as miR-NC). The transfection was performed using Lipofectamine 2000 according to the manufacturer's instruction (Invitrogen).

Analysis of miR-149 and Puma by Quantitative Reverse Transcription-PCR (qRT-PCR)—qRT-PCR was carried out according to the previously described method (24). miR-149 levels were measured by qRT-PCR using a TaqMan® MicroRNA Assays kit according to the manufacturer's instructions in an ABI Prism 7000 sequence detection system (Applied Biosystems). Total RNA was extracted using TRIzol reagent. After DNase I (Takara) treatment, RNA was reverse-transcribed with reverse transcriptase (ReverTra Ace, Toyobo). The results of qRT-PCR were normalized to that of U6. The sequences of U6 primers were forward 5′-GCTTCGGCAGCACATATACTAA-3′ and reverse 5′-AACGCTTCACGAATTTGCGT-3′. qRT-PCR analysis for Puma was performed using the SYBR Green Real Time PCR Master Mix (Takara) according to the manufacturer's instructions. The data analyzed by qRT-PCR were normalized to that of mouse glyceraldehyde-3-phosphate dehydrogenase (GAPDH). The sequences of Puma primers were forward 5′-AGGAGGGGGTCTGTGAAGAG-3′ and reverse 5′-CTGGGCACTGGGTTAAGAAG-3′. The sequences of mouse GAPDH primers were forward 5′-TGTGTCCGTCGTGGATCTGA-3′ and reverse 5′-CCTGCTTCACCACCTTCTTGA-3′.

Northern Blot Analysis—To detect miR-149, the probes were labeled with the nonradioactive digoxigenin using an End Tailing Kit (Roche Applied Science). 15 μg of total RNA were loaded onto a precast 15% denaturing TBE-urea polyacrylamide gel and transferred by electroblotting to Nybond N+ (GE Healthcare). After UV cross-linking, the membrane was hybridized with digoxigenin-labeled probes. The probe sequence used against miR-149 was 5′-GGGAGTGAAGACACGGAGCCAGA-3′. The hybridizations and washes were performed using an Ultrahyb-Oligo buffer (Ambion) at 42 °C according to the manufacturer's instructions. The detections were achieved by the alkaline phosphatase-conjugated anti-digoxigenin antibody (Roche Applied Science) and the CDP-Star reagent (GE Healthcare).

Reporter Constructions and Luciferase Assay—3′UTR of Puma was amplified from mouse genomic DNA. The primers for Puma 3′UTR amplification were 5′-TCCGCCTTCTGACACCCT-3′ and 5′-AACCACTGAGCCATTTCT-3′. To generate reporter vector bearing miR-149-binding sites, 3′UTR of Puma was cloned into the pGL3 vector (Promega) immediately downstream of the stop codon of the luciferase gene. The mutated 3′UTR was generated, and mutation (the wild type Puma 3′UTR, GCCA; the mutated Puma 3′UTR, AGGC) was introduced into the binding site. For luciferase assay, cells in 24-well plates were co-transfected with the plasmid constructs of 200 ng/per well of empty pGL3, pGL3 harboring the wild type 3′UTR (pGL3-Puma-WT-3′UTR), or the mutated 3′UTR (pGL3-Puma-MUT-3′UTR) of Puma, along with 60 nmol/liter miR-149 using Lipofectamine 2000 (Invitrogen). pRL-TK vector containing *Renilla* luciferase cDNA served as the internal control. Mimic control (miR-NC) served as a negative control. 36 h after transfection, cells were lysed, and luciferase activity was measured with the Dual-Luciferase kit (Promega) according to the manufacturer's instructions.

Adenovirus Construction and Infection—Adenoviruses harboring the coding sequence of Puma without 3′UTR (Puma-W/O-3′UTR) and Puma with mutated 3′UTR (Puma-MUT-3′UTR) were constructed using the Adeno-X Expression System (Clontech) according to the manufacturer's instructions. The mutations were introduced to the binding site of miR-149 on Puma 3′UTR. CCAG in the wild type Puma 3′-UTR were converted to AGCA using QuikChange II XL site-directed mutagenesis kit (Stratagene). Adenoviral Puma with 3′UTR (Puma-W-3′UTR) and adenoviral β-galactosidase (β-gal) were used as we described (21). To construct adenoviruses encoding the A-allelic (miR-149-A) and G-allelic pre-miR-149 (miR-149-G), the same sequences cloned into pcDNA3.0 above were amplified and finally cloned into the adenoviral system. Adenoviruses encoding Cel-miR-39 was constructed using the same system. Viruses were amplified in HEK293 cells. Cells were infected with the viruses at the indicated multiplicity of infection (m.o.i.) for 1 h. After washing with PBS, the culture medium was added, and cells were cultured until the indicated time.

Preparation of RNAi Construct of Puma—The RNAi constructs were designed using the siRNA Design Tools from Ambion. Puma RNAi (Si-Puma) sense sequence was 5′-CCTGGAGGGTCATGTACAATCTCTT-3′; Si-Puma antisense sequence was 5′-AAGAGATTGTACATGACCCTCCAGG-3′. The scramble Puma-siRNA (Scr-Puma) sense sequence was 5′-TACATCATTGTCGTGCTGCGAGTCA-3′; Scr-Puma antisense sequence was 5′-TGACTCGCAGCACGACAATGATGTA-3′. They were cloned into pSilencer adeno 1.0-CMV vector (Ambion) according to the manufacturer's instructions. The specificity of the oligonucleotides was confirmed by comparison with all other sequences in GenBank™ using Nucleotide BLAST. There was no homology to other known mouse DNA sequences.

TUNEL Assay—Cells were fixed in 4% paraformaldehyde in PBS and permeabilized with 0.1% Triton X-100 in 0.1% sodium citrate. An *in situ* apoptotic cell death detection kit (fluorescein, Roche Applied Science) based on TUNEL assay was used as per the manufacturer's instructions to detect apoptotic cells. Negative controls were included in each case by omitting TUNEL enzyme terminal deoxynucleotidyltransferase reaction mixture and incubating the cells with the label solution. PBS containing 5 μg/ml 4′,6′-diamidino-2-phenylindole (DAPI; Vector Laboratories) was prepared to stain nuclei. Sections were examined with a Zeiss LSM510 META microscope. The percentage of apoptotic nuclei was calculated. 100–150 cells were counted in 20–30 random fields. For apoptosis analysis by TUNEL assay in heart sections, the procedure was the same except that cardiomyocytes were stained with the α-actinin antibody (A7811, Sigma). An investigator blind to the treatment quantified 20 random fields of samples.

Immunoblotting—Immunoblotting was performed as we reported earlier (25). In brief, cells were lysed for 1 h at 4 °C in a lysis buffer (20 mmol/liter Tris (pH 7.5), 2 mmol/liter EDTA, 3 mmol/liter EGTA, 2 mmol/liter DTT, 250 mmol/liter sucrose, 0.1 mmol/liter phenylmethylsulfonyl fluoride (PMSF), 1% Triton X-100, and a protease inhibitor mixture). Samples were subjected to 12% SDS-PAGE and transferred to nitrocellulose membranes. Equal protein loading was controlled by Ponceau red staining of membranes. Blots were probed using primary

antibodies. Anti-Puma antibody (Abcam) was used at the ratio of 1:200. Anti-actin antibody (Santa Cruz Biotechnology) was used at 1:2000. After four washes with PBS/Tween 20, horseradish peroxidase-conjugated secondary antibodies were added. Antigen-antibody complexes were visualized by enhanced chemiluminescence.

Caspase-3 Activity Assay—Caspase-3 activity was measured using an Apo-ONE homogeneous caspase-3/7 assay kit (Promega) according to the manufacturer's protocol. Briefly, Apo-ONE caspase-3/7 reagent was added, and the mixtures were incubated at room temperature for up to 6 h. The level of fluorescence was measured using a Synergy 4 Hybrid Microplate Reader (BioTek Instruments) with excitation/emission at 499/521 nm.

Mitochondrial Staining and Immunofluorescence—Cells were plated onto the coverslips coated with 0.01% poly-L-lysine. After treatment they were stained for 20 min with 0.02 μmol/liter MitoTracker Red CMXRos (Molecular Probes). Immunofluorescence was performed as we described previously (25). The samples were imaged using a laser scanning confocal microscope (Zeiss LSM 510 META).

Animal Studies—We obtained C57BL/6 mice from the Institute of Laboratory Animal Science of the Chinese Academy of Medical Sciences (Beijing, China). Myocardial ischemic model was established by ligating left anterior descending of the coronary artery to cause myocardial ischemia as we described previously (24). Briefly, mice were anesthetized and placed on an HX-300S animal ventilator. Body temperature was maintained at 37 °C on a heating pad. The beating heart was accessed via a small left anterior thoracotomy. After removing the pericardium, a descending branch of the left anterior descending coronary artery was ligated with a nylon suture. Ligation was confirmed by the whitening of a region of the left ventricle. Adenoviral miR-149-A, miR-149-G, or β-gal was injected immediately after left anterior descending ligation into the myocardium bordering the infarct zone at a dose of 1×10^{11} viral genome particles per animal using an insulin syringe with a small gauge needle, respectively. The chest was closed, and the animals were moved back to cages after the occurrence of spontaneous breathing. Cardiac function of these groups of animals was evaluated by echocardiographic analysis 14 days after the surgery. Trichrome stain of the heart section was performed by employing the trichrome stain (MASSON) kit HT-15 (Sigma).

Statistical Analysis—Pearson's χ^2 test was used to evaluate the differences in the distribution of genotypes between cases and controls. Hardy-Weinberg equilibrium was assessed using a goodness-of-fit χ^2 test. Association between the miR-149 polymorphism and the risk of myocardial infarction was analyzed by multivariate unconditional logistic regression, adjusted for gender, age, hypertension, and diabetes status. All analyses were performed using SPSS software (version 13.0, SPSS). All measurement data are shown as means ± S.D. or means ± S.E. of at least three independent experiments. Statistical analyses of the differences between groups were conducted by one-way analysis of variance followed by the LSD post hoc test for multiple comparisons. Paired data were evaluated by Student's t test. $p < 0.05$ was considered statistically significant.

RESULTS

miR-149 Polymorphism rs71428439 Is Associated with the Risk for MI—We analyzed the samples of myocardial infarction and the controls, and their characteristics were summarized in Table 1, including gender, age, hypertension, and diabetes status. The observed genotype distribution of the miR-149 rs71428439 polymorphism in both cases and control groups was in agreement with Hardy-Weinberg equilibrium ($p = 0.312$ and $p = 0.659$, respectively), indicating no population stratification within the cohort. We observed that the genotype distribution of this polymorphism in myocardial infarction cases was statistically significantly different from that in control subjects ($\chi^2 = 12.639$ and $p = 0.002$). The GG genotype in the patients was remarkably more frequent than that in the controls. A similar trend was also observed in the frequency of the AG genotype (Table 2). The association between the genotype and the risk of myocardial infarction was further analyzed using multivariate unconditional logistic regression with adjustment for gender, age, hypertension, and diabetes status. We observed a statistically significant association of the GG phenotype with the increased risk for myocardial infarction (before adjustment, odds ratio (OR) = 2.340, 95% confidence interval (CI) = 1.448–3.783, $p = 0.001$; after adjustment, OR = 2.323, 95% CI =

TABLE 1
Base-line characteristics of the samples

	Controls ($n = 296$)	MI ($n = 289$)	p value
Age (years)[a]	58.49 ± 14.33	60.51 ± 12.90	0.075
Gender (men/women)[b]	214/82	224/65	0.146
Hypertension[b]	27 (9.12%)	38 (13.15%)	0.121
Diabetes mellitus[b]	19 (6.42%)	24 (8.30%)	0.382

[a] p values were calculated by Student's t test.
[b] p values were calculated by Pearson's χ^2 test.

TABLE 2
The association between miR-149 SNP rs71428439 and the risk for MI

Genotype	Control ($n = 296$) no.	MI ($n = 289$) no.	Before adjustment		After adjustment	
			OR[a] (95% CI)	p values[a]	OR[b] (95% CI)	p values[b]
	%	%				
AA	132 (44.6%)	95 (32.9%)	1 (Reference)		1 (Reference)	
AG	126 (42.6%)	130 (45.0%)	1.408 (0.982–2.017)	0.050	1.427 (0.993–2.051)	0.055
GG	38 (12.8%)	64 (22.1%)	2.340 (1.448–3.783)	0.001	2.323 (1.432–3.770)	0.001
AA	132 (44.6%)	95 (32.9%)	1 (Reference)		1 (Reference)	
AG+GG	164 (55.4%)	194 (67.1%)	1.644 (1.175–2.300)	0.004	1.635 (1.165–2.293)	0.004
AA+AG	258 (87.2%)	225 (77.9%)	1 (Reference)		1 (Reference)	
GG	38 (12.8%)	64 (22.1%)	1.931 (1.245–2.997)	0.003	1.922 (1.235–2.993)	0.004

[a] OR means odds ratio. OR and p values were calculated by multivariate unconditional logistic regression before adjustment for gender, age, hypertension, and diabetes status.
[b] OR and p values were calculated by multivariate unconditional logistic regression after adjustment for gender, age, hypertension and diabetes status.

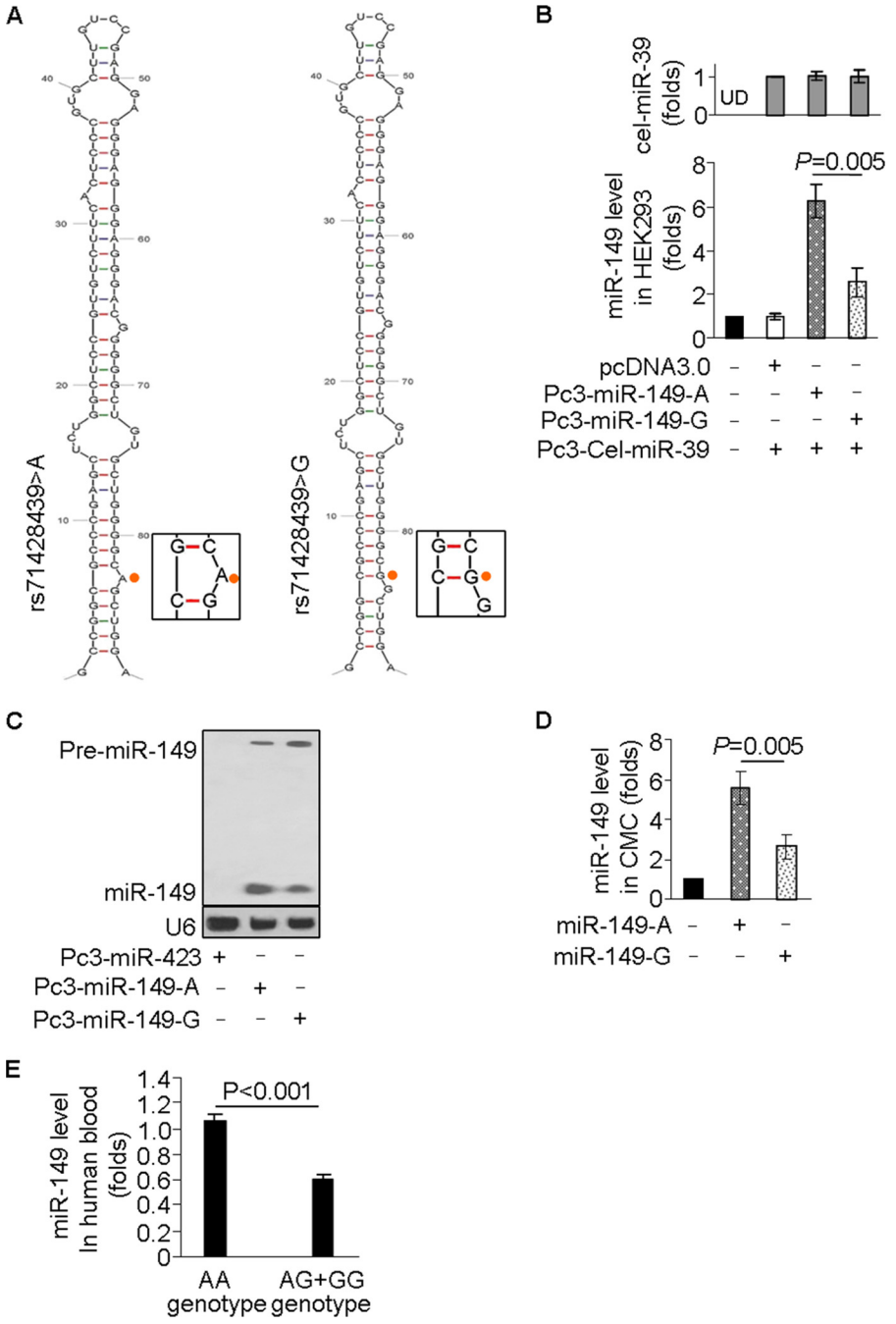

FIGURE 1. **rs71428439 polymorphism affects the maturation of miR-149.** *A,* hairpin loop structure of the A- and G-allelic miR-149 precursor is different. The polymorphism site is indicated by the *dots*. The A→G polymorphism located in the stem region outside of the mature miR-149 sequence causes a change to the stem structure of the precursor. *B* and *C,* G allele shows a low level of mature miR-149 compared with the A allele in HEK293 cells. HEK293 cells were transfected with the plasmids of empty pcDNA3.0, pc3.0-miR-149-A, pc3.0-miR-149-G, or pc3.0-miR-423 along with pc3.0-cel-miR-39, respectively. 24 h after transfection, miR-149 and cel-miR-39 levels were analyzed by qRT-PCR (*B*). For Northern blot, the miR-149 precursor and mature miR-149 were indicated (*C*). A representative result of three independent experiments is shown. *UD*, undetectable. *D,* G allele impairs miR-149 maturation in cardiomyocytes (*CMC*). Cardiomyocytes were infected with adenoviral miR-149-A or miR-149-G, respectively. 24 h after infection, miR-149 levels were analyzed by qRT-PCR. The qRT-PCR results were normalized to that of U6. *E,* levels of miR-149 in human peripheral blood mononuclear cells. The qRT-PCR results were normalized to that of U6 levels. Data are shown as means ± S.E. (n = 29–35).

1.432–3.770, p = 0.001) as shown in Table 2. Moreover, the ORs for myocardial infarction risk were higher in the recessive model (after adjustment, GG *versus* AA+AG, OR = 1.922, and 95% CI = 1.235–2.993) than that in the dominant model (after adjustment, GG +AG *versus* AA, OR = 1.635, and 95% CI = 1.165–2.293), indicating a recessive role of the G allele for the prognostication of myocardial infarction risk.

rs71428439 Polymorphism Affects the Maturation of miR-149—To detect the consequence of SNP rs71428439 bringing to miR-149, we used the mfold web server to predict the minimum free-energy secondary structure of pre-miR-149-A and pre-miR-149-G and found that the G allele causes a difference to the structure of pre-miR-149 from the A allele (Fig. 1*A*). Sequence-mediated differences in processing miRNAs have

been reported (12, 27). We thus explored whether the SNP could influence the processing of mature miR-149. To this end, HEK293 cells were transfected with pcDNA3.0-pre-miR-149-A (pc3-miR-149-A) or pcDNA3.0-pre-miR-149-G (pc3-miR-149-G), along with a plasmid expressing *Caenorhabditis elegans* miR-39 (cel-miR-39, which shares no homologous sequence in human and mouse) as a control of transfection and expression efficiency. Real time PCR was used to detect the effect of different alleles on the expression levels of mature miR-149. As shown in Fig. 1*B*, the expression levels of mature miR-149 from the G allele were less than that from the A allele.

To further confirm these results, Northern blot was used to detect the expression levels of miR-149 between the different alleles. We utilized the cells transfected with pcDNA3.0-pre-miR-423 plasmids as a control to exclude the influence of foreign sequence on miR-149 levels. The amount of miR-149 was also observed to be diverse between the different alleles. The expression levels of mature miR-149 from the G allele were lower than that from the A allele (Fig. 1*C*). To test whether the polymorphism would also affect miR-149 maturation in cardiomyocytes, we infected cells with adenoviral pre-miR-149-A (miR-149-A) or pre-miR-149-G (miR-149-G) and observed that pre-miR-149-G still produced less mature miR-149 than pre-miR-149-A in cardiomyocytes (Fig. 1*D*). These *in vitro* results prompted us to examine the association between rs71428439 genotypes and mature miR-149 expression levels in human samples. There were significantly lower levels of mature miR-149 in human peripheral blood mononuclear cells from people with at least one G allele (AG or GG genotype) in genome than from those with the A allele (AA genotype) (Fig. 1*E*). These data suggest that the G to A substitution in pre-miR-149 attenuates the processing of mature miR-149.

miR-149 Inhibits Apoptosis—To understand the function of miR-149, we used chemically synthesized 2′-OMe-oligonucleotides (AS-miR-149), the sequence of which is complementary to mature miR-149, to knock down endogenous miR-149. The scramble oligonucleotides were used as a negative control (designated as AS-NC). AS-miR-149 could efficiently reduce endogenous miR-149 levels (Fig. 2*A*). At first, we assessed the effects of H_2O_2 on endogenous miR-149 expression. The cells were exposed to a dose range of H_2O_2 at different time points. miR-149 levels were reduced in a time- and dose-dependent manner (Fig. 2, *B* and *C*). TUNEL analysis revealed that knockdown of miR-149 caused the cells to be more susceptible to apoptosis upon hydrogen peroxide treatment (Fig. 2*D*). In addition, miR-149 knockdown promoted caspase 3 activation induced by H_2O_2 (Fig. 2*E*).

Then we tested whether ectopic expression of miR-149 can influence apoptosis. miRNA duplex was used for miRNA overexpression. Principally, the miR-149 duplex (miR-149) contained an RNA strand with a sequence identical to the mature miR-149 and an artificial strand that was partially complementary to the mature miR-149 sequence. miR-NC, used as a negative control, was an miRNA duplex with a scrambled sequence that was nonhomologous to any mouse genome sequence. miR-149 levels were observed to increase by the administration of miR-149 duplex but not miR-NC (Fig. 2*F*). miR-149 could significantly attenuate caspase 3 activation and apoptosis induced by H_2O_2 (Fig. 2, *G* and *H*). These data suggest that miR-149 is able to inhibit apoptosis.

To know the biological consequences of impaired processing of miR-149, we tested whether the A to G variation caused by SNP could influence apoptosis. To know whether the consequence brought by SNP can be disturbed by infection or expression efficiency, the infection/expression efficiency was monitored through co-infection with Cel-miR-39, and the levels of mature miR-149 were detected (Fig. 2*I*). Adenoviruses harboring pre-miR-149 with the A allele elicited a stronger effect on the inhibition of caspase 3 activation and apoptosis than the one with the G allele (Fig. 2, *J* and *K*). Thus, it appears that there is a functional effect of the SNP.

Puma Is a Target of miR-149—miRNAs execute their functions through inhibiting translation or promoting degradation of their target mRNAs. To work out the molecular mechanisms by which miR-149 regulates apoptosis, we searched the potential targets of miR-149 using the program of targetscan. Puma has a conservative miR-149-binding site in its 3′UTR (Fig. 3*A*). We observed that the mRNA and protein levels of Puma were increased responding to H_2O_2 treatment (Fig. 3, *B* and *C*). The administration of AS-miR-149 resulted in an elevated Puma protein levels (Fig. 3*D*). Enforced expression of miR-149 attenuated the increase in Puma levels upon H_2O_2 treatment (Fig. 3*E*). These data suggest that miR-149 participates in regulating Puma expression.

To learn whether Puma is a direct target of miR-149, we created luciferase constructs of Puma with a wild type 3′UTR (pGL3-WT-Puma-3′UTR) and with a mutated 3′UTR (pGL3-MUT-Puma-3′UTR). Luciferase reporter assays revealed that miR-149 induced a decrease in the luciferase activity of pGL3-WT-Puma-3′UTR but not pGL3-MUT-Puma-3′UTR (Fig. 3*F*). H_2O_2 increased the activity of luciferase constructs containing the Puma wild type 3′UTR (Puma-WT-3′UTR), and this increase was attenuated by miR-149. However, this effect could not be observed in Puma mutated 3′UTR (Puma-MUT-3′UTR) (Fig. 3*G*). Moreover, pc3-miR-149-A caused many more reductions in the luciferase activity of pGL3-WT-Puma-3′UTR than pc3-miR-149-G (Fig. 3*H*). In addition, we infected the cells with adenoviruses containing Puma with wild type 3′UTR (Puma-W-3′UTR), with mutated 3′UTR (Puma-MUT-3′UTR), or without 3′UTR (Puma-W/O-3′UTR) (Fig. 3*I*). Immunoblot showed that miR-149 could subdue the expression of Puma with 3′UTR but not Puma without 3′UTR or Puma with mutated 3′UTR (Fig. 3*J*). Next, we infected the cells with adenoviral Puma-W-3′UTR along with adenoviral miR-149-A or miR-149-G. The infection/expression efficiency and the levels of miR-149 were detected (Fig. 3*K*). miR-149-A repressed Puma expression at a greater degree than miR-149-G (Fig. 3*L*). These data indicate that miR-149 directly regulates Puma expression, and the SNP rs71428439 is able to influence the effect of pre-miR-149 on the expression levels of Puma.

Puma Regulates Mitochondrial Network—To explore the underlying mechanism by which Puma initiates the apoptotic program, we produced Puma siRNA (Si-Puma) and its scrambled form (Scramble). Si-Puma but not its scrambled form could abrogate H_2O_2-induced Puma expression (Fig. 4*A*).

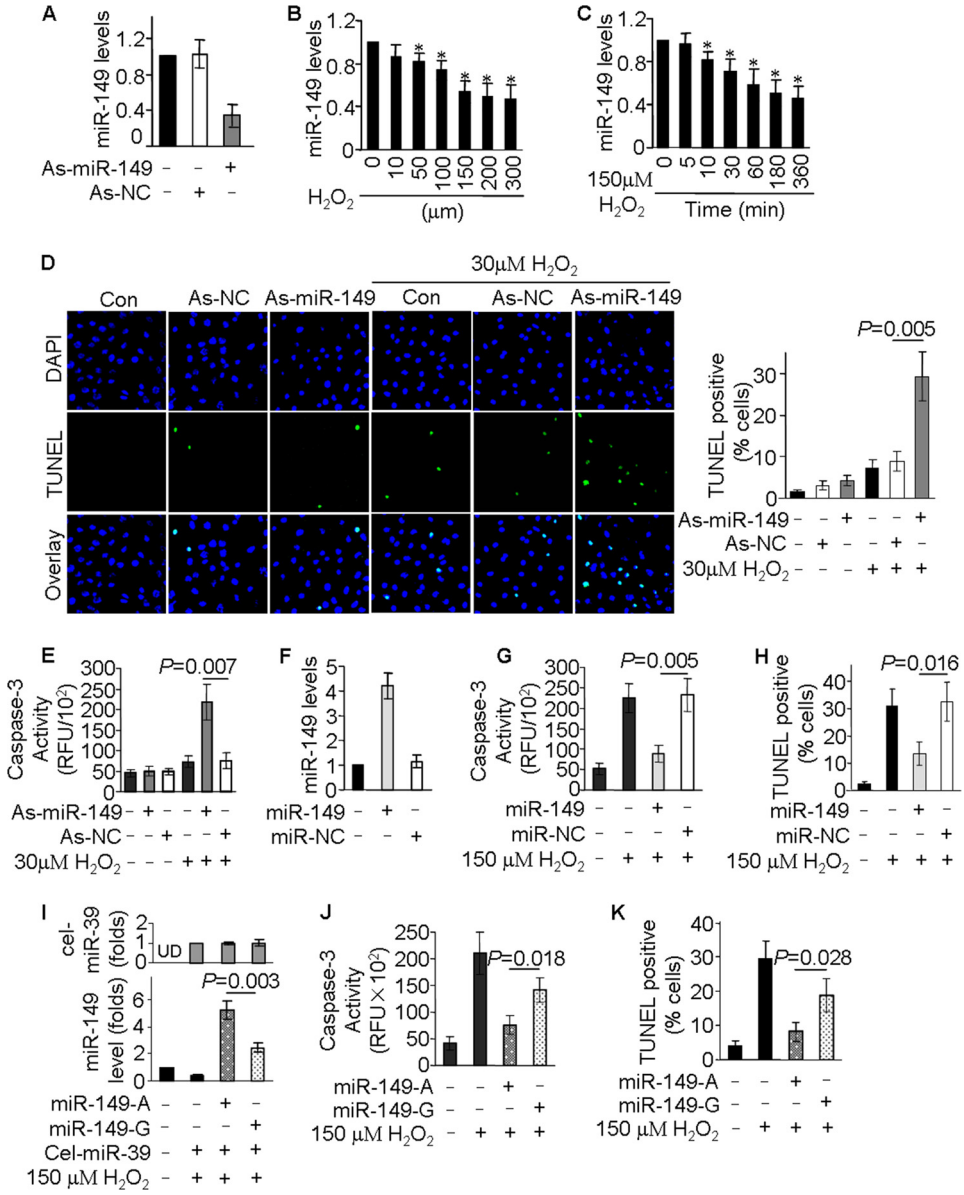

FIGURE 2. **miR-149 inhibits apoptosis.** *A,* miR-149 antagomir can efficiently reduce endogenous miR-149 levels. Cardiomyocytes were transfected with miR-149 antagomir (*As-miR-149*) or antagomir negative control (*As-NC*). Data are expressed as the mean ± S.D. of three independent experiments. *B* and *C,* mature miR-149 decreases upon treatment with H_2O_2. The cardiomyocytes were treated with the indicated concentrations of H_2O_2 and harvested after 1 h (*B*) or treated with 150 μM H_2O_2 and harvested at the indicated times (*C*) for the detection of miR-149 level using qRT-PCR. The results were normalized to that of U6. Data are expressed as the mean ± S.D. of three independent experiments. *, $p < 0.05$ *versus* control. *D,* knockdown of endogenous miR-149 renders cells more sensitive to H_2O_2-induced apoptosis. Cardiomyocytes were transfected with As-miR-149 or As-NC. 24 h after transfection, they were exposed to 30 μM H_2O_2 for 6 h. The TUNEL assay was utilized to detect apoptosis. Quantitative analysis of apoptosis is shown in *right panel*. Data are expressed as the mean ± S.D. of three independent experiments. *Con*, control. *E,* knockdown of endogenous miR-149 elevates caspase-3 activities upon H_2O_2 treatment. Cells were treated as described for *D*. Data are expressed as the mean ± S.D. of three independent experiments. *F,* miR-149 mimic elevates the levels of miR-149. Cardiomyocytes were transfected with miR-149 mimic (*miR-149*) or negative control (*miR-NC*). 24 h after transfection, miR-149 levels were detected. Data are expressed as the mean ± S.D. of three independent experiments. *G,* miR-149 blocks the activation of caspase-3 induced by H_2O_2. Cardiomyocytes were transfected with miR-149 or miR-NC. After 24 h, cells were exposed to 150 μM H_2O_2 for 6 h, and caspase-3 activity was analyzed. Data are expressed as the mean ± S.D. of three independent experiments. *H,* miR-149 attenuates H_2O_2-induced apoptosis. Cells were treated as for *G*. Cell apoptosis was analyzed by TUNEL assay. Data are expressed as the mean ± S.D. of three independent experiments. *I,* infection/expression efficiency and levels of miR-149 were monitored. Cardiomyocytes were infected with adenoviruses harboring miR-149 precursor with the A allele (*miR-149-A*) or the G allele (*miR-149-G*), along with adenoviruses harboring cel-miR-39 precursor. After 24 h, cells were treated with 150 μM H_2O_2 for 6 h. miR-149 and cel-miR-39 levels were detected by qRT-PCR. The results were normalized to that of U6. *UD,* undetectable,. *J* and *K,* G-allelic miR-149 precursor suppresses caspase-3 activation and apoptosis at a lesser degree compared with the A-allelic one. Cardiomyocytes were infected with adenoviruses harboring the miR-149 precursor with the A allele (*miR-149-A*) or the G allele (*miR-149-G*) at a, m.o.i. of 50. After 24 h, cells were treated with 150 μM H_2O_2 for 6 h and harvested for the analysis of caspase 3 activities (*J*) and apoptosis (*K*). Data are expressed as the mean ± S.D. of three independent experiments.

Enforced expression of Puma could initiate mitochondrial fission, whereas knockdown of Puma attenuated mitochondrial fission induced by H_2O_2 treatment (Fig. 4*B*). Puma overexpression promoted caspase 3 activation, and the abrogation of Puma impaired caspase 3 activation induced by H_2O_2 treatment (Fig. 4*C*). Concomitantly, overexpression of Puma induced apoptosis, whereas knockdown of Puma abolished apoptosis caused by H_2O_2 stimulation (Fig. 4*D*). These results

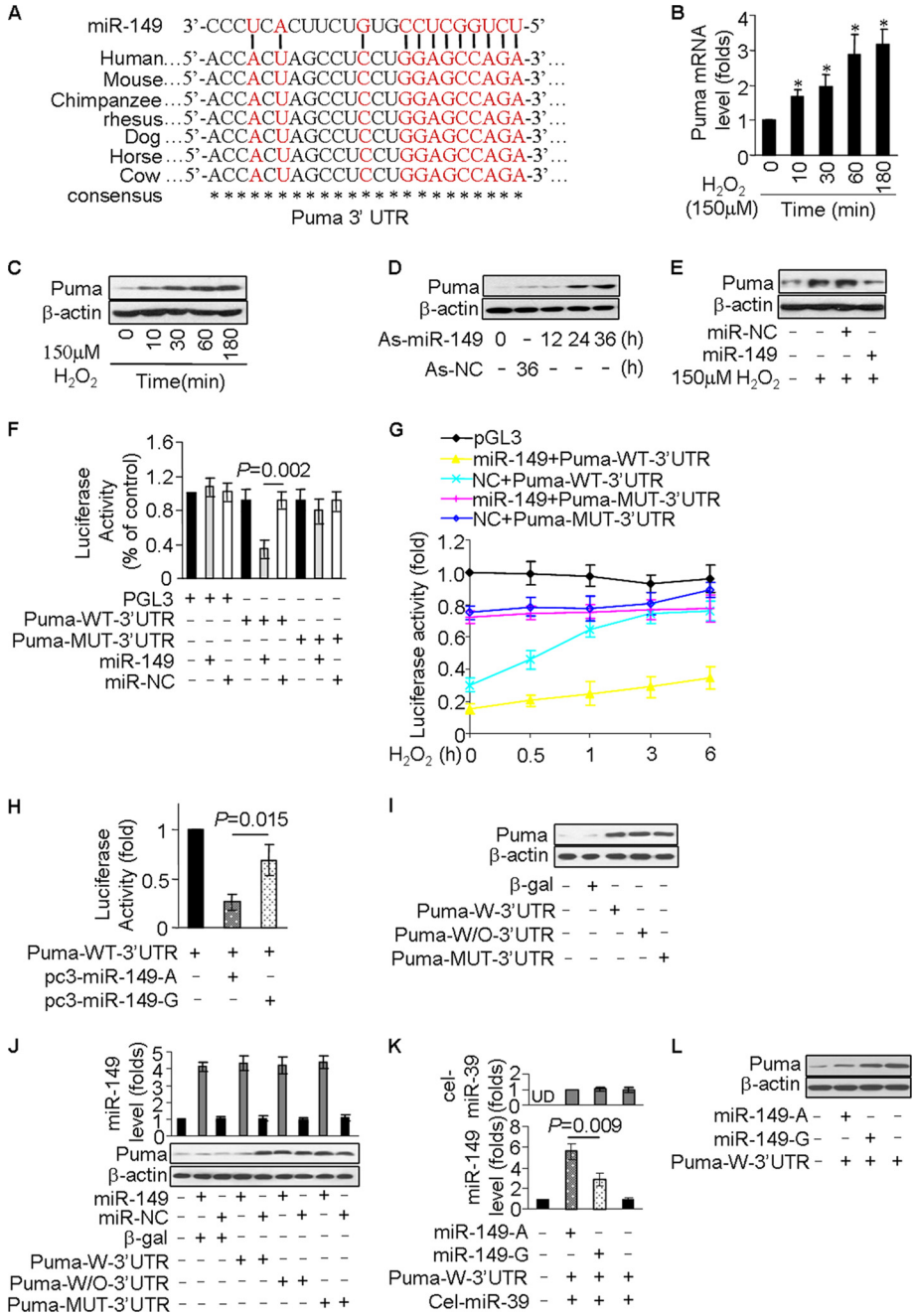

FIGURE 3. **Puma is a direct target of miR-149.** *A,* sequence alignment of putative miR-149 targeting site in 3′UTR of Puma shows a high level of complementary and sequence conservation. *B* and *C,* Puma is up-regulated upon treatment with H_2O_2. Cardiomyocytes were treated with 150 μM H_2O_2. At the indicated times, cells were harvested for the analysis of Puma mRNA levels by RT-PCR (*B*) or protein levels by immunoblot (*C*). *, $p < 0.05$ *versus* control. Data are expressed as the mean ± S.D. of three independent experiments. *D,* inhibition of endogenous miR-149 leads to a marked increase of Puma. Cardiomyocytes were treated with As-miR-149 and harvested at the indicated times. Puma protein levels were analyzed by immunoblot. A representative blot of three independent experiments is shown. *E,* miR-149 attenuates the increase of endogenous Puma induced by H_2O_2. Cardiomyocytes were transfected with miR-149 and after 24 h were exposed to 150 μM H_2O_2 for 6 h. Puma levels were analyzed by immunoblot. *F,* miR-149 inhibits Puma translation. HEK293 cells were transfected with the luciferase constructs of the wild type Puma-3′UTR (Puma-WT-3′UTR) or the mutated Puma-3′UTR (Puma-MUT-3′UTR), along with miR-149 or miR-NC. Luciferase activity was measured after 36 h. Data are expressed as the mean ± S.D. of three independent experiments. *G,* miR-149 abrogates the increase of Puma translation activity. Cardiomyocytes were transfected with miR-149 or miR-NC, along with the luciferase construct Puma-WT-3′UTR or Puma-MUT-3′UTR, and exposed to 150 μM H_2O_2. Luciferase activity was measured at the indicated times. Data are expressed as the mean ± S.D. of three independent experiments. *H,* G-allelic pre-miR-149 causes a lesser reduction of Puma translation activity than the A-allelic one. HEK293 cells were transfected with the Puma-WT-3′UTR luciferase construct, along with the expression plasmids pc-miR-149-A or pc-miR-149-G. Luciferase activity was measured after 36 h. Data are expressed as the mean ± S.D. of three independent experiments. *I,* analysis of Puma expression. Cardiomyocytes were infected with adenoviral β-gal or Puma with 3′UTR (*Puma-W-3′UTR*) or without 3′UTR (*Puma-W/O-3′UTR*) at an m.o.i. of 100. Puma was analyzed by immunoblot. *J,* miR-149 inhibits the expression of Puma with 3′UTR but not without 3′UTR or with mutated 3′UTR. Cardiomyocytes were infected with adenoviral β-gal, Puma-W-3′UTR, Puma-W/O-3′UTR, or Puma-MUT-3′UTR at an m.o.i. of 100 and were transfected with miR-149 or miR-NC. miR-149 levels and Puma were analyzed by qRT-PCR or immunoblot, respectively. *K,* infection/expression efficiency and maturation of miR-149 were detected. Cardiomyocytes were infected with adenoviral miR-149-A or miR-149-G, along with adenoviral Puma with 3′UTR and adenoviral cel-miR-39. miR-149 levels were detected by qRT-PCR. *UD,* undetectable. *L,* G-allelic pre-miR-149 suppresses the expression of Puma at a lesser degree than the A-allelic one. Cardiomyocytes were infected with adenoviral miR-149-A or miR-149-G at an m.o.i. of 50, along with adenoviral Puma with 3′UTR at an m.o.i. of 100. After 30 h of infection, Puma protein levels were detected by immunoblot. A representative blot of three independent experiments is shown.

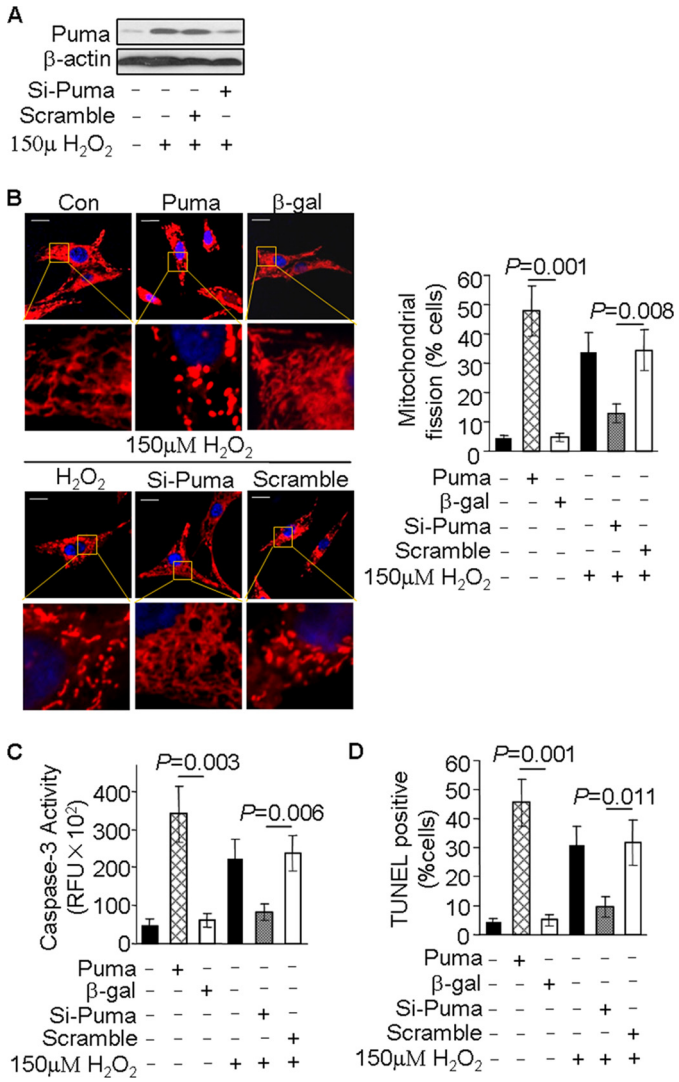

FIGURE 4. **Puma regulates mitochondrial network.** *A,* Puma siRNA efficiently attenuates Puma levels. Cardiomyocytes were infected with adenoviruses harboring Puma RNAi (*Si-Puma*) or its scrambled form (*Scramble*) at an m.o.i. of 100. 24 h after infection, cells were exposed to 150 μM H_2O_2 for 6 h and harvested for the analysis of Puma levels by immunoblot. A representative blot of three independent experiments is shown. *B,* Puma promotes mitochondrial fission. Cardiomyocytes were infected with adenoviral Puma, β-gal, Si-Puma, or Scramble. After 24 h, cells infected with adenoviral Si-Puma or Scramble were exposed to 150 μM H_2O_2 for 6 h. Representative photos show mitochondrial fission (*left*). *Con,* control. *Bar,* 10 μm. The percentages of cells undergoing mitochondrial fission were counted (*right*). Data are expressed as the mean ± S.D. of three independent experiments. *C,* Puma activates caspase-3. Cells were treated as for *B*. Caspase-3 activity was analyzed. Data are expressed as the mean ± S.D. of four independent experiments. *D,* Puma promotes apoptosis. Cardiomyocytes were treated as for *B*. The percentages of apoptotic cells were counted and analyzed. Data are expressed as the mean ± S.D. of four independent experiments.

indicate a critical role for Puma in regulating mitochondrial network and apoptosis responding to H_2O_2 induction.

Puma Is Required for miR-149 to Control Mitochondrial Network and Apoptosis—We examined the relationship between Puma and miR-149 in regulating the mitochondrial network and apoptosis. As shown in Fig. 5*A*, the inhibition of endogenous miR-149 could elevate caspase 3 activation induced by H_2O_2. When Puma was knocked down, inhibition of miR-149 failed to promote caspase 3 activation induced by H_2O_2. Intriguingly, miR-149 inhibition could promote mitochondrial fission and apoptosis, and this effect was abolished upon knockdown of Puma (Fig. 5*B*), suggesting that Puma is a target of miR-149 in regulating mitochondrial network and apoptosis.

To test whether Puma is a direct or indirect target of miR-149 in eliciting its effect, we employed the constructs of adenoviral Puma-W-3′UTR and Puma-W/O-3′UTR. miR-149 significantly reduced caspase 3 activity induced by Puma-W-3′UTR but not Puma-W/O-3′UTR (Fig. 5*C*). Concomitantly, miR-149 could significantly decrease mitochondrial fission and apoptosis induced by Puma-W-3′UTR but failed to attenuate mitochondrial fission and apoptosis caused by Puma-W/O-3′UTR (Fig. 5*D*). To test whether the SNP could elicit effects on apoptosis, we infected cells with adenoviral miR-149-A or miR-149-G. It was observed that compared with miR-149-A, miR-149-G caused a lesser reduction of caspase 3 activation (Fig. 5*E*), mitochondrial fission, and apoptosis (Fig. 5*F*) induced by enforced expression of Puma with wild type 3′UTR. These data suggest that Puma is a direct target of miR-149 in regulating the mitochondrial network and that the allelic G impairs the ability of pre-miR-149 to repress the mitochondrial network and apoptosis.

Inverse Expression of miR-149 and Puma in Ischemia—Finally, we attempted to know the expression levels of miR-149 and Puma under the pathological conditions. The pathophysiology of myocardial infarction involves a reduced blood supply to the myocardium. Ischemia can induce cardiomyocyte apoptosis (28). We tested their levels in the ischemic conditions. miR-21 has been verified to be highly expressed in the heart (20). By comparing with miR-21 expression levels in the heart, miR-149 was observed to possess relatively high expression levels in the heart under physiological conditions (Fig. 6*A*). However, miR-149 showed a low level in the area at risk in the ischemic heart (Fig. 6*B*). In contrast, Puma increased under ischemic conditions (Fig. 6*B*). Taken together, these results suggest that miR-149 and Puma show an inverse expression level in ischemia.

A and G Allele of rs71428439 Polymorphism Affects Myocardial Infarction in Mouse Models—We assessed whether miR-149 can influence myocardial infarction and cardiac function. Puma was increased markedly after the MI surgery, which was much more attenuated by miR-149-A than miR-149-G (Fig. 7*A*). The cardiac functions were more significantly preserved in the mice receiving miR-149-A (Fig. 7*B*). The infarct size was much reduced in mice receiving miR-149-A (Fig. 7*C*). Consistently, mice receiving miR-149-A displayed a lower degree of myocyte apoptosis (Fig. 7*D*). The results in the mouse model motivated us to further compare the clinical features of the MI patients based on the miR-149 SNP genotype. It was observed that fractional shortening in patients carrying the G allele in the genome was significantly lower than that of patients carrying the A allele (Fig. 7*E*). Together, the results indicate that the SNP rs71428439 is able to influence the effect of pre-miR-149 on myocardial infarction.

DISCUSSION

SNPs in miRNA genes, including pri-miRNAs, pre-miRNAs, and mature miRNAs, may influence the processing and/or target selection of miRNAs. In this study, we first showed that SNP rs71428439 located in miR-149 precursor can affect the expression of miR-149. In particular, it is associated with cardiac

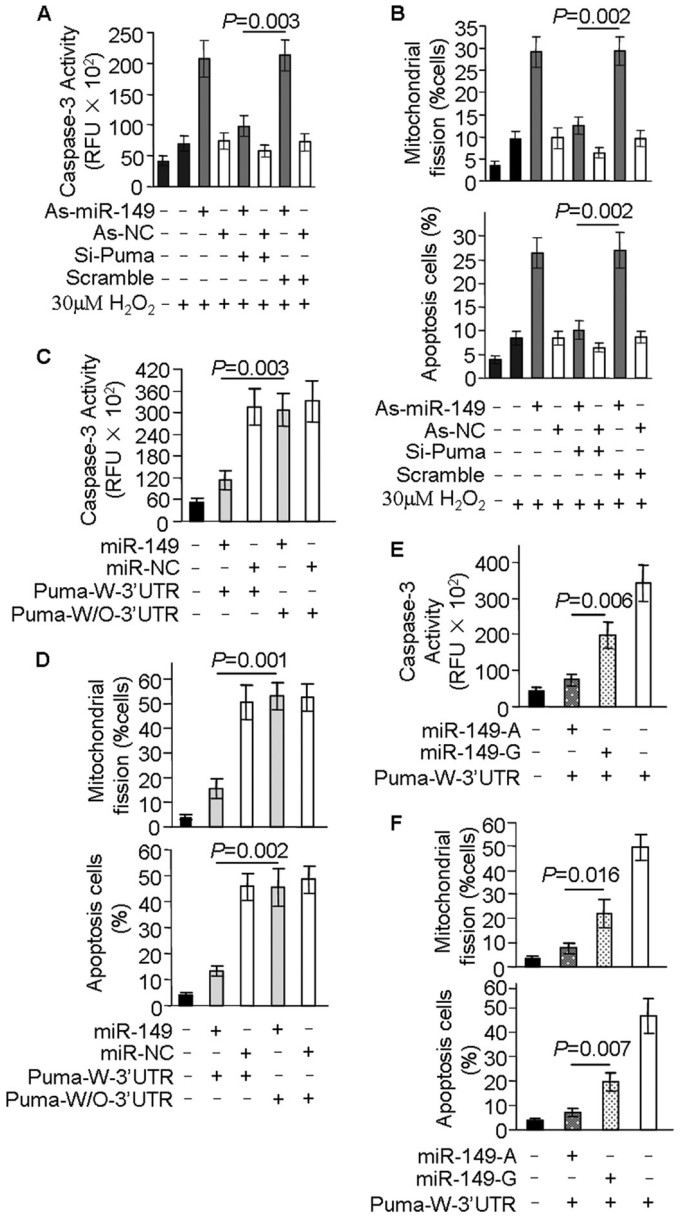

FIGURE 5. **Puma is required for miR-149 to control mitochondrial network and apoptosis.** *A,* Puma siRNA abrogates caspase-3 activation caused by knockdown of miR-149. Cardiomyocytes were infected with adenoviruses harboring Puma siRNA or its scrambled form at an m.o.i. of 100 and transfected with As-miR-149 or As-NC. After 24 h, cells were exposed to 30 μM H_2O_2 for 6 h. Caspase-3 activity was analyzed. Data are expressed as the mean ± S.D. of three independent experiments. *B,* knockdown of Puma blocks mitochondrial fission and apoptosis induced by miR-149 inhibition. Cells were treated as for *A*. Mitochondrial fission (*upper panel*) and apoptosis (*low panel*) were analyzed. Data are expressed as the mean ± S.D. of three independent experiments. *C,* miR-149 inhibits caspase-3 activation induced by Puma with 3′UTR but not Puma without 3′UTR. Cardiomyocytes were transfected with miR-149 or miR-NC and infected with adenoviral Puma-W-3′UTR or Puma-W/O-3′UTR at an m.o.i. of 100. 30 h later, cells were collected for the analysis of caspase-3 activity. Data are expressed as the mean ± S.D. of three independent experiments. *D,* miR-149 abrogates mitochondrial fission and apoptosis induced by Puma with 3′UTR but not Puma without 3′UTR. Cells were treated as for *C*. The percentages of mitochondrial fission (*upper panel*) and apoptosis (*low panel*) were analyzed. Data are expressed as the mean ± S.D. of three independent experiments. *E,* G-allelic pre-miR-149 exerts a lesser effect on caspase-3 activation induced by Puma than the A-allelic one. Cardiomyocytes were infected with adenoviral miR-149-A or miR-149-G at an m.o.i. of 50, along with adenoviral Puma with 3′UTR at an m.o.i. of 100. 30 h after infection, caspase-3 activity was analyzed. Data are expressed as the mean ± S.D. of three independent experiments. *F,* A- and G-allelic pre-miR-149 abrogate mitochondrial fission and apoptosis induced by Puma at a significantly different degree. Cardiomyocytes were treated as for *E*. The percentages of mitochondrial fission (*upper panel*) and apoptosis (*low panel*) were analyzed. Data are expressed as the mean ± S.D. of three independent experiments.

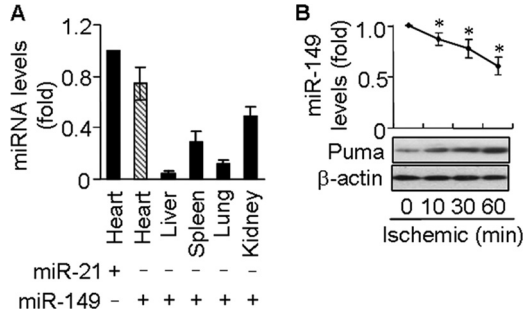

FIGURE 6. **Inverse expression of miR-149 and Puma in ischemic myocardial tissue.** *A,* endogenous miR-149 is highly expressed in mouse heart. miR-149 level was detected in different mouse organs by RT-PCR. The data were normalized to U6. miR-149 levels were compared with miR-21 levels in mouse heart ($n = 6$). *B,* expression of miR-149 and Puma are inversely related during myocardial ischemia. The areas at risk were collected at the indicated ischemic time. miR-149 levels were analyzed by RT-PCR ($n = 6$), *, $p < 0.05$ *versus* control. Puma was analyzed by immunoblot.

infarction. In exploring the underlying molecular mechanism, we found that Puma is a target of miR-149. The reduced expression of miR-149 leads to the up-regulation of Puma in response to apoptotic stimulation. miR-149 regulates mitochondrial fission and apoptosis through Puma. Our results reveal a novel model of SNP that can affect mitochondrial dynamics.

Although the association between the SNPs in protein-coding genes and the risk of myocardial infarction has been extensively investigated, there are few reports showing that myocardial infarction is in association with the SNPs in miRNA genes. This study demonstrates that the rare allele of SNP rs71428439 located in miR-149 precursor is closely associated with the risk of myocardial infarction. We observed that the individuals with GG genotype of miR-149 gene are at a higher risk for myocardial infarction compared with the individuals with the AA genotype. Intriguingly, we found that an A to G variation in the miR-149 precursor caused by SNP rs71428439 affects the production of mature miR-149. The G-allelic pre-miR-149 exhibits a lower expression level of mature miR-149 compared with the A-allelic one. This effect may have stemmed from the minimal free-energy secondary structure change of the precursor caused by the A to G variation. A growing body of evidence demonstrates that the integrity of the precursor RNA stem is required for mature miRNA production. For example, the introduction of artificial mutations on the miR-30 precursor are detrimental to mature miR-30 processing (29). It has been reported that the polymorphism rs2910164 located in the stem region of miR-146a precursor influences the production of mature miR-146a (12, 30). The G to U variation in the miR-125a precursor results in a reduced production of mature miR-125a (16).

We investigated the biological function of miR-149 and found that miR-149 can conquer mitochondrial related apoptosis through targeting the pro-apoptotic protein Puma. The suppression of miR-149 renders cardiomyocytes more sensitive to undergo apoptosis, although the enforced expression of miR-149 reduces apoptosis. The miRNAs execute their functions by inhibiting their target gene expression (31). This work for the

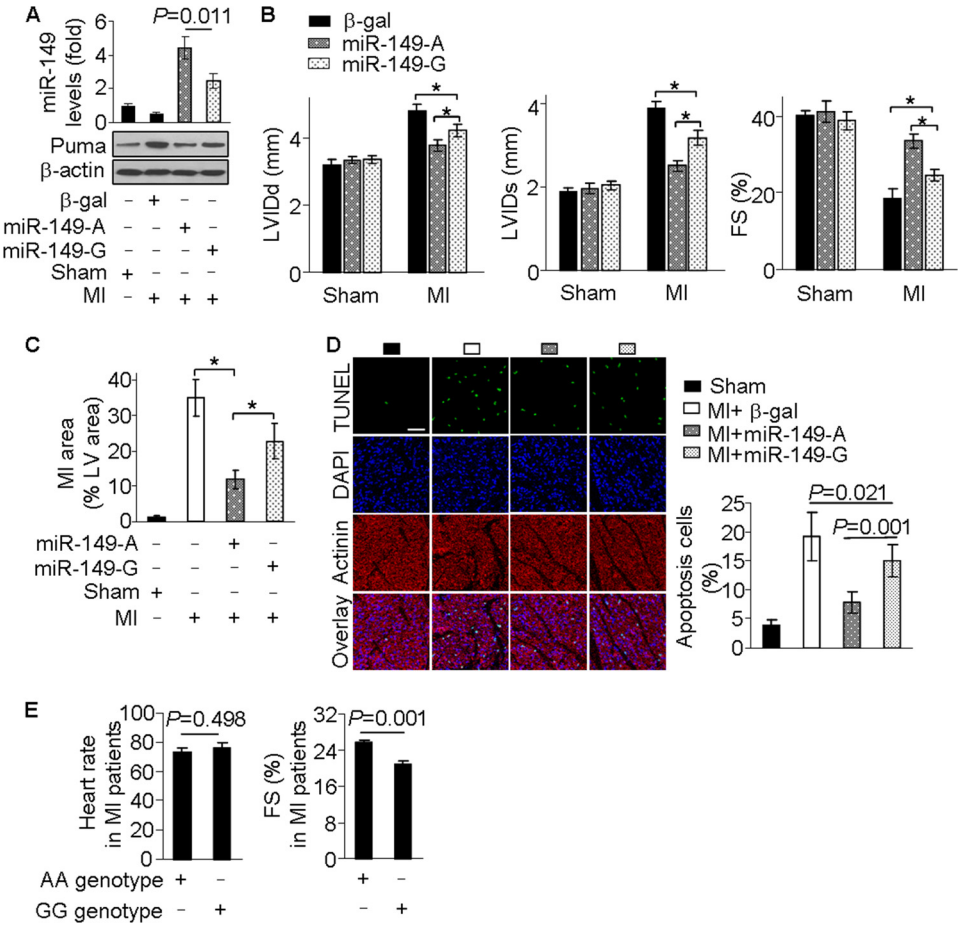

FIGURE 7. **rs71428439 polymorphism effects on myocardial infarction.** *A,* analysis of miR-149 and Puma levels under myocardial infarction. Adult male C57 mice (8–10 weeks old) were injected with adenoviral β-gal, miR-149-A, or miR-149 and subjected to permanent left anterior descending coronary artery ligation. miR-149 levels were analyzed by qRT-PCR. Puma was analyzed by immunoblot. *B,* A and G alleles of rs71428439 polymorphism exert differential effect on cardiac function. Mice were treated as in *A*. Cardiac functions were evaluated by echocardiography. $n = 8$ per group. *C,* A and G alleles of rs71428439 polymorphism exert differential effect on myocardial infarction sizes. Mice were treated as in *A*. MI areas were calculated as the ratio of MI area to left ventricular (*LV*) area. $n = 6–8$ mice per group. *, $p < 0.05$. *D,* analysis of apoptosis by TUNEL assay in mice. *Green,* TUNEL-positive nuclei; *blue,* DAPI-stained nuclei; *red,* cardiomyocytes labeled with the antibody to α-actinin; *scale bar,* 50 μm. *Bar graph* shows quantitative analysis of apoptosis. $n = 5–6$ mice per group. *E,* analysis of cardiac function of MI patients based on miR-149 rs71428439 genotype. *FS,* fractional shortening. Data are shown as means ± S.E. ($n = 49–82$).

first time shows that miR-149 modulates Puma expression in cardiomyocytes. Puma belongs to the Bcl-2 homology 3-only subfamily of Bcl-2-related pro-apoptotic proteins. Recently, it was reported that Puma is required for cardiac cell death upon ischemia/reperfusion in mouse hearts (32). Puma null mice are significantly resistant to ischemia-reperfusion injury. The infarct sizes in the Puma-null hearts are reduced by 50% compared with the wild type or heterozygous mice. Also, Puma is verified to participate in mediating cardiomyocyte apoptosis induced by endoplasmic reticulum stress (33). In this study, we observed that the expression of Puma is negatively regulated by miR-149.

Mitochondria constantly undergo fusion and fission, two necessary processes for the maintenance of organelle fidelity (34). However, the abnormal mitochondrial fission is involved in the initiation of apoptosis (35–37). We have previously shown that miRNAs can regulate mitochondrial fission and apoptosis in cardiomyocytes by targeting mitochondrial fission proteins (24). In this study, we have found that miR-149 prevents mitochondrial fission in cardiomyocytes, and it regulates mitochondrial fission by targeting Puma. Puma is exclusively located to mitochondria. It is necessary to find out the molecular mechanism by which Puma regulates mitochondrial fission in a future study.

A recent report has summarized the myocardial infarction-related miRNAs, and miR-149 is one of them (38), but the underlying mechanism remains largely unknown. This study offered evidence to support the point that miR-149 may play a vital role in controlling apoptosis during myocardial infarction. Furthermore, this work revealed that the A- and G-allelic miR-149 precursors display an obvious difference in their abilities to regulate apoptosis. A sudden insufficient blood supply to the myocardium is a major reason of myocardial infarction, resulting in a loss of cardiomyocytes. Cellular apoptosis is one typical pathological feature of myocardial infarction. Our data suggest that the SNP rs71428439 executes functional influence on apoptosis by conferring different levels of miR-149, which causes the different levels of Puma.

miR-149 has been reported to be down-regulated both in mice heart tissue and human heart tissue of MI (39). In this study, we explored the role of miR-149-Puma axis in myocardial infarction in the mouse model. The employment of human

heart samples harboring the SNP rs71428439 in the genome can further strengthen this finding.

Noticeably, besides Rs71428439, Rs3746444 in has-mir-499, Rs6505162 in has-miR-423, and Rs2292832 in has-miR-149 have also been detected in this study. Rs2292832 in has-miR-149 has been reported to be involved in susceptibility with gastric cancer risk (40), head and neck squamous cell carcinoma risk (41), as well as coal workers' pneumoconiosis risk (26). However, only Rs71428439 in has-miR-149 was observed to be associated with the risk of MI in our study.

In summary, this work revealed that miR-149 SNP may affect its function in regulating apoptosis. Identifying more new miRNA SNP sites and exploring their mechanisms will greatly improve our knowledge of the etiology of diseases and provide a useful tool for creating efficient individualized treatment for complicated diseases.

REFERENCES

1. Nora, J. J., Lortscher, R. H., Spangler, R. D., Nora, A. H., and Kimberling, W. J. (1980) Genetics–epidemiologic study of early-onset ischemic heart disease. *Circulation* **61,** 503–508
2. Musunuru, K., and Kathiresan, S. (2010) Genetics of coronary artery disease. *Annu. Rev. Genomics Hum. Genet.* **11,** 91–108
3. Musunuru, K., Strong, A., Frank-Kamenetsky, M., Lee, N. E., Ahfeldt, T., Sachs, K. V., Li, X., Li, H., Kuperwasser, N., Ruda, V. M., Pirruccello, J. P., Muchmore, B., Prokunina-Olsson, L., Hall, J. L., Schadt, E. E., Morales, C. R., Lund-Katz, S., Phillips, M. C., Wong, J., Cantley, W., Racie, T., Ejebe, K. G., Orho-Melander, M., Melander, O., Kotliansky, V., Fitzgerald, K., Krauss, R. M., Cowan, C. A., Kathiresan, S., and Rader, D. J. (2010) From noncoding variant to phenotype via SORT1 at the 1p13 cholesterol locus. *Nature* **466,** 714–719
4. Fischer, M., Broeckel, U., Holmer, S., Baessler, A., Hengstenberg, C., Mayer, B., Erdmann, J., Klein, G., Riegger, G., Jacob, H. J., and Schunkert, H. (2005) Distinct heritable patterns of angiographic coronary artery disease in families with myocardial infarction. *Circulation* **111,** 855–862
5. Marenberg, M. E., Risch, N., Berkman, L. F., Floderus, B., and de Faire, U. (1994) Genetic susceptibility to death from coronary heart disease in a study of twins. *N. Engl. J. Med.* **330,** 1041–1046
6. Bartel, D. P. (2004) MicroRNAs: genomics, biogenesis, mechanism, and function. *Cell* **116,** 281–297
7. O'Connell, R. M., Rao, D. S., Chaudhuri, A. A., and Baltimore, D. (2010) Physiological and pathological roles for microRNAs in the immune system. *Nat. Rev. Immunol.* **10,** 111–122
8. Thum, T., Catalucci, D., and Bauersachs, J. (2008) MicroRNAs: novel regulators in cardiac development and disease. *Cardiovasc. Res.* **79,** 562–570
9. Nelson, P. T., Wang, W. X., and Rajeev, B. W. (2008) MicroRNAs (miRNAs) in neurodegenerative diseases. *Brain Pathol.* **18,** 130–138
10. Tomankova, T., Petrek, M., and Kriegova, E. (2010) Involvement of microRNAs in physiological and pathological processes in the lung. *Respir. Res.* **11,** 159
11. Ji, R., Cheng, Y., Yue, J., Yang, J., Liu, X., Chen, H., Dean, D. B., and Zhang, C. (2007) MicroRNA expression signature and antisense-mediated depletion reveal an essential role of MicroRNA in vascular neointimal lesion formation. *Circ. Res.* **100,** 1579–1588
12. Jazdzewski, K., Murray, E. L., Franssila, K., Jarzab, B., Schoenberg, D. R., and de La Chapelle, A. (2008) Common SNP in pre-miR-146a decreases mature miR expression and predisposes to papillary thyroid carcinoma. *Proc. Natl. Acad. Sci. U.S.A.* **105,** 7269–7274
13. Horikawa, Y., Wood, C. G., Yang, H., Zhao, H., Ye, Y., Gu, J., Lin, J., Habuchi, T., and Wu, X. (2008) Single nucleotide polymorphisms of microRNA machinery genes modify the risk of renal cell carcinoma. *Clin. Cancer Res.* **14,** 7956–7962
14. Hu, Z., Liang, J., Wang, Z., Tian, T., Zhou, X., Chen, J., Miao, R., Wang, Y., Wang, X., and Shen, H. (2009) Common genetic variants in pre-microRNAs were associated with increased risk of breast cancer in Chinese women. *Hum. Mutat.* **30,** 79–84
15. Chin, L. J., Ratner, E., Leng, S., Zhai, R., Nallur, S., Babar, I., Muller, R. U., Straka, E., Su, L., and Burki, E. A. (2008) A SNP in a let-7 microRNA complementary site in the KRAS 3′untranslated region increases non-small cell lung cancer risk. *Cancer Res.* **68,** 8535–8540
16. Duan, R., Pak, C., and Jin, P. (2007) Single nucleotide polymorphism associated with mature miR-125a alters the processing of pri-miRNA. *Hum. Mol. Genet.* **16,** 1124–1131
17. Dorn, G. W., 2nd, Matkovich, S. J., Eschenbacher, W. H., and Zhang, Y. (2012) A human 3′miR-499 mutation alters cardiac mRNA targeting and function, novelty and significance. *Circ. Res.* **110,** 958–967
18. Sayed, D., Hong, C., Chen, I. Y., Lypowy, J., and Abdellatif, M. (2007) MicroRNAs play an essential role in the development of cardiac hypertrophy. *Circ. Res.* **100,** 416–424
19. Sun, Y. Q., Koo, S., White, N., Peralta, E., Esau, C., Dean, N. M., and Perera, R. J. (2004) Development of a micro-array to detect human and mouse microRNAs and characterization of expression in human organs. *Nucleic Acids Res.* **32,** 22, e188
20. Cheng, Y., Ji, R., Yue, J., Yang, J., Liu, X., Chen, H., Dean, D. B., and Zhang, C. (2007) MicroRNAs are aberrantly expressed in hypertrophic heart–Do they play a role in cardiac hypertrophy? *Am. J. Pathol.* **170,** 1831–1840
21. Murtaza, I., Wang, H. X., Feng, X., Alenina, N., Bader, M., Prabhakar, B. S., and Li, P. F. (2008) Down-regulation of catalase and oxidative modification of protein kinase CK2 lead to the failure of apoptosis repressor with caspase recruitment domain to inhibit cardiomyocyte hypertrophy. *J. Biol. Chem.* **283,** 5996–6004
22. Li, Y. Z., Lu, D. Y., Tan, W. Q., Wang, J. X., and Li, P. F. (2008) p53 initiates apoptosis by transcriptionally targeting the antiapoptotic protein ARC. *Mol. Cell. Biol.* **28,** 564–574
23. Lim, L. P., Lau, N. C., Garrett-Engele, P., Grimson, A., Schelter, J. M., Castle, J., Bartel, D. P., Linsley, P. S., and Johnson, J. M. (2005) Microarray analysis shows that some microRNAs down-regulate large numbers of target mRNAs. *Nature* **433,** 769–773
24. Wang, J. X., Jiao, J. Q., Li, Q., Long, B., Wang, K., Liu, J. P., Li, Y. R., and Li, P. F. (2011) miR-499 regulates mitochondrial dynamics by targeting calcineurin and dynamin-related protein-1. *Nat. Med.* **17,** 71–78
25. Wang, J. X., Li, Q., and Li, P. F. (2009) Apoptosis repressor with caspase recruitment domain contributes to chemotherapy resistance by abolishing mitochondrial fission mediated by dynamin-related protein-1. *Cancer Res.* **69,** 492–500
26. Wang, M., Ye, Y., Qian, H., Song, Z., Jia, X., Zhang, Z., Zhou, J., and Ni, C. (2010) Common genetic variants in pre-microRNAs are associated with risk of coal workers' pneumoconiosis. *J. Hum. Genet.* **55,** 13–17
27. Qi, L., Hu, Y., Zhan, Y., Wang, J., Wang, B. B., Xia, H. F., and Ma, X. (2012) An SNP site in pri-miR-124 changes mature miR-124 expression but no contribution to Alzheimer's disease in a Mongolian population. *Neurosci. Lett.* **515,** 1–6
28. Kusano, K. F., Pola, R., Murayama, T., Curry, C., Kawamoto, A., Iwakura, A., Shintani, S., Ii, M., Asai, J., and Tkebuchava, T. (2005) Sonic hedgehog myocardial gene therapy: tissue repair through transient reconstitution of embryonic signaling. *Nat. Med.* **11,** 1197–1204
29. Zeng, Y., and Cullen, B. R. (2003) Sequence requirements for micro RNA processing and function in human cells. *RNA* **9,** 112–123
30. Xu, T., Zhu, Y., Wei, Q. K., Yuan, Y., Zhou, F., Ge, Y. Y., Yang, J. R., Su, H., and Zhuang, S. M. (2008) A functional polymorphism in the miR-146a gene is associated with the risk for hepatocellular carcinoma. *Carcinogenesis* **29,** 2126–2131
31. Zhang, C. (2008) MicroRNomics: a newly emerging approach for disease biology. *Physiol. Genomics* **33,** 139–147
32. Toth, A., Jeffers, J. R., Nickson, P., Min, J. Y., Morgan, J. P., Zambetti, G. P., and Erhardt, P. (2006) Targeted deletion of Puma attenuates cardiomyocyte death and improves cardiac function during ischemia-reperfusion. *Am. J. Physiol. Heart Circ. Physiol.* **291,** H52–H60
33. Nickson, P., Toth, A., and Erhardt, P. (2007) PUMA is critical for neonatal cardiomyocyte apoptosis induced by endoplasmic reticulum stress. *Cardiovasc. Res.* **73,** 48–56
34. Tanaka, A., and Youle, R. J. (2008) A chemical inhibitor of DRP1 uncouples mitochondrial fission and apoptosis. *Mol. Cell* **29,** 409–410

35. McBride, H. M., Neuspiel, M., and Wasiak, S. (2006) Mitochondria: more than just a powerhouse. *Curr. Biol.* **16,** R551–R560
36. Frank, S., Gaume, B., Bergmann-Leitner, E. S., Leitner, W. W., Robert, E. G., Catez, F., Smith, C. L., and Youle, R. J. (2001) The role of dynamin-related protein 1, a mediator of mitochondrial fission, in apoptosis. *Dev. Cell* **1,** 515–525
37. Li, Q., Zhou, L.-Y., Gao, G.-F., Jiao, J.-Q., and Li, P.-F. (2012) Mitochondrial network in the heart. *Protein Cell* **3,** 410–418
38. Liu, Z., Yang, D., Xie, P., Ren, G., Sun, G., Zeng, X., and Sun, X. (2012) MiR-106b and MiR-15b modulate apoptosis and angiogenesis in myocardial infarction. *Cell. Physiol. Biochem.* **29,** 851–862
39. van Rooij, E., Sutherland, L. B., Thatcher, J. E., DiMaio, J. M., Naseem, R. H., Marshall, W. S., Hill, J. A., and Olson, E. N. (2008) Dysregulation of microRNAs after myocardial infarction reveals a role of miR-29 in cardiac fibrosis. *Proc. Natl. Acad. Sci. U.S.A.* **105,** 13027–13032
40. Zhang, M. W., Jin, M. J., Yu, Y. X., Zhang, S. C., Liu, B., Jiang, X., Pan, Y. F., Li, Q. I., Ma, S. Y., and Chen, K. (2012) Associations of lifestyle-related factors, hsa-miR-149 and hsa-miR-605 gene polymorphisms with gastrointestinal cancer risk. *Mol. Carcinog.* **51,** E21–E31
41. Tu, H.-F., Liu, C.-J., Chang, C.-L., Wang, P.-W., Kao, S.-Y., Yang, C.-C., Yu, E.-H., Lin, S.-C., and Chang, K.-W. (2012) The association between genetic polymorphism and the processing efficiency of miR-149 affects the prognosis of patients with head and neck squamous cell carcinoma. *PLoS One* **7,** e51606